

Experimental evidence for Luttinger liquid behavior in sufficiently long GaAs V-groove quantum wires

E. Levy,^{1,*} I. Sternfeld,¹ M. Eshkol,¹ M. Karpovski,¹ B. Dwir,² A. Rudra,² E. Kapon,² Y. Oreg,³ and A. Palevski¹

¹*School of Physics and Astronomy, Raymond and Beverly Sackler Faculty of Exact Sciences, Tel Aviv University, Tel Aviv 69978, Israel*

²*Ecole Polytechnique Federale de Lausanne (EPFL), Laboratory of Physics of Nanostructures, CH-1015 Lausanne, Switzerland*

³*Department of Condensed Matter Physics, The Weizmann Institute of Science, Rehovot 76100, Israel*

(Received 8 November 2011; revised manuscript received 20 December 2011; published 18 January 2012)

We have measured the temperature dependence of the conductance of long V-groove quantum wires fabricated using GaAs/AlGaAs heterostructures, in a wide temperature range ($200 \text{ mK} < T < 4.2 \text{ K}$). We find that for our quantum wires the Fermi velocity can be as low as $v_F \cong 5 \times 10^4 \text{ m/s}$, corresponding to an interaction parameter value of $g \cong 0.56$. This value suggests that our data are consistent with theories developed within the framework of the Luttinger liquid model in the presence of a single strong barrier (*weak link*).

DOI: [10.1103/PhysRevB.85.045315](https://doi.org/10.1103/PhysRevB.85.045315)

PACS number(s): 73.21.Hb, 71.10.Pm

I. INTRODUCTION

It is known that the electronic conductance through noninteracting clean quantum wires (QWRs) is quantized in units of the universal value $2e^2/h$,¹ as was observed in quantum point contact constrictions in a two-dimensional electron gas (2DEG).^{2,3} In these short and clean wires, there is no interaction between electrons and the conductance is temperature independent. However, in longer QWRs ($L \gg \lambda_F$), electron-electron ($e-e$) interactions play a significant role. These interactions are included within the framework of the Luttinger liquid (LL) model,⁴⁻⁷ in which the conductance of the 1D system decreases with the temperature T , given that there is disorder in the system. For sufficiently *weak disorder*, theories predict that the conductance is very close to the universal value $2e^2/h$, with a small (negative) correction which depends on the temperature as $T^{(g-1)}$.⁸⁻¹² Here, g is a parameter which is a measure of the strength of the interactions. Such LL behavior has been experimentally observed in carbon nanotubes¹³⁻¹⁶ and semiconductor QWRs.¹⁷⁻¹⁹

On the other hand, for systems containing *stronger disorder*, the temperature dependence of the conductance is expected to be much stronger. For such systems, the value of the conductance for each populated channel is not close to the universal value, and in general is not well defined due to the specific realization of the disorder potential, so that perturbation theory is inapplicable. Therefore, one should use other theories, concerning *weak links*,^{8,9} stronger disorder due to many impurities,²⁰ or stronger backscattering.²¹

Kane and Fisher^{8,9} have found that the conductance through a *weak link* (single strong barrier) depends on the temperature in the following power-law manner:

$$G(T) \propto \left(\frac{T}{T_0}\right)^{\left(\frac{1}{g}-1\right)}, \quad (1)$$

where g is the dimensionless interaction parameter, as before, which depends on the ratio between the Coulomb energy U and the Fermi energy E_F and which is given by the following expression:

$$g = (1 + U/2E_F)^{-1/2}. \quad (2)$$

Another known form of Eq. (2) is $g = (1 + 2\alpha)^{-1/2}$.²² The dimensionless parameter α is another commonly used

interaction parameter which depends on the electron charge density and therefore on the Fermi velocity.²³ For repulsive interactions, $g < 1$, and as interactions become stronger, the value of g decreases ($g = 1$ means no interactions). Therefore, the conductance of the system is predicted to vanish as $T \rightarrow 0$, since the power in Eq. (1) is always positive for repulsive interactions. The other parameter, T_0 , is a measure of the strength of the disorder in the system.

Gornyi *et al.*²⁰ claim that the conductance through a system containing many impurities should exhibit a stronger temperature dependence. They have shown that as the temperature is lowered, the system enters the so-called *strongly localized regime* (where the phase-coherence length becomes longer than the localization length, $L_\phi \gtrsim \xi$). This happens at temperature $T_1 = T_\xi/\alpha^2$, where $k_B T_\xi = 1/\nu\xi$, and ν is the density of states. In this regime, the conductance is predicted to decrease with decreasing temperature, first linearly, and as the temperature is further decreased (at temperature $T_3 = T_\xi/\alpha$) a stronger temperature dependence is predicted. At a lower temperature $T_c \sim T_\xi/\alpha \ln \alpha^{-1}$, the system undergoes a localization transition below which the conductance vanishes, namely, $G(T < T_c) = 0$. The critical behavior above T_c is

$$\ln G(T) \propto -(T - T_c)^{-1/2}, \quad (3)$$

as $T \rightarrow T_c$.

The value of g (or α) is thus important for both theories: It determines the power in Eq. (1) and can be compared with known values obtained for GaAs (~ 0.7 in the limit of weak disorder¹⁷⁻¹⁹). Moreover, it determines the temperature scales given in the many-impurities theory, and especially T_ξ .

In this work, we present an experimental study of the temperature dependence of the conductance of sufficiently long V-groove GaAs QWRs. Our results are consistent with theories developed within the framework of the LL model in the presence of a weak link, for which we obtain that the interaction parameter can be as low as $g \cong 0.56$ ($\alpha \cong 1$).

II. SAMPLE PREPARATION AND THE MEASUREMENT SETUP

The QWRs studied here were produced by low-pressure (20 mbar) metal-organic vapor-phase epitaxy (MOVPE) of GaAs/AlGaAs heterostructures on undoped (001) GaAs

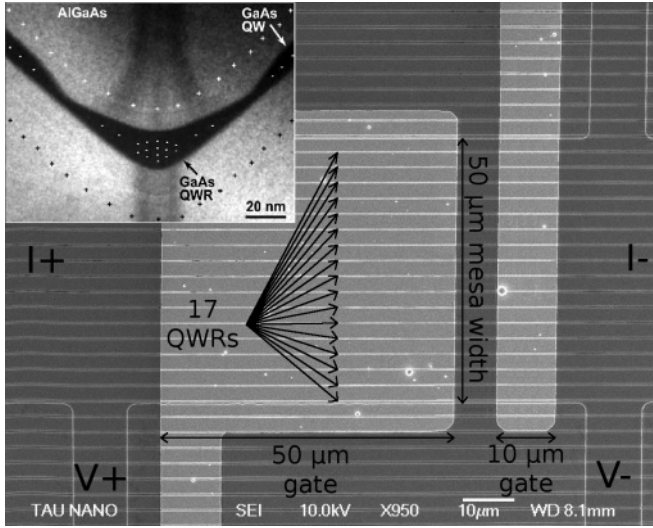


FIG. 1. A top view scanning electron microscope image of a typical sample of many V grooves connected in parallel. The horizontal lines are the bottoms of the V grooves. Two Schottky gates, with lengths of 10 and 50 μm , are deposited over the mesa. Application of negative gate voltage to a gate enables measurement of a set of 17 macroscopically identical QWRs which are classically connected in parallel (see text). The conductance was measured by the four-terminal method, in which the current was passed in two probes (denoted as $I+$ and $I-$), while the voltage was measured at two other probes ($V+$ and $V-$). Inset: Cross-sectional transmission electron microscope image of a single V-groove QWR, on which the charge distribution is schematically shown.

substrates patterned with V grooves oriented in the $[01\bar{1}]$ direction, fabricated by lithography and wet chemical etching.²⁴ Gratings with $3\mu\text{m}$ pitch were used. The details about the growth are similar to those reported elsewhere.¹⁷ The inset of Fig. 1 shows a transmission electron microscope image of the heterostructure grown on a single V groove, on which the charge distribution is schematically depicted.

The samples were fabricated using standard photolithography techniques with a $50\text{-}\mu\text{m}$ -wide mesa etched along the QWRs. Each sample consists 17 V grooves connected in parallel. Contact to the 2DEG regions was provided by connecting the sample to source and drain Au/Ge/Ni pads. Top Ti/Au Schottky gates of various widths were formed in order to isolate the QWRs and control the number of populated 1D subbands in them. The 1D QWR at the bottom of each groove is electrostatically connected to the 2DEG quantum wells (QWs) on the sidewalls (see inset of Fig. 1) through the narrowest parts (expressed by an energetic barrier), so that the transport in the system is carried by both the electrons in the QWs and those in the QWRs. In order to isolate and measure only QWR segments we use the depletion technique. By applying negative gate voltage (V_G), electrons are depleted from both QWs and QWRs. Full depletion at the QWs occurs before the QWRs are emptied due to the fact that the conduction band of the QWRs lies lower in energy than that of the QWs. Further increase in the negative voltage will continue depleting electrons from the QWRs. Note that the width of the gate determines the length of the QWRs realized underneath it.²⁵ Thus, for each sample we measure a set of 17 macroscopically

identical QWRs of the same length, which are classically connected in parallel. The wires are distant from each other ($3\mu\text{m}$ between neighboring wires) so that correlation effects are irrelevant. As was mentioned in our previous work,¹⁷ the disorder in V-groove QWRs stems mainly from interface roughness brought about by lithography imperfections on the patterned substrate and peculiar faceting taking place during MOVPE on a nonplanar surface.²⁶ The specific features of the disorder in the QWRs studied here, in terms of the depth and size of the localization potential, are expected to vary from sample to sample. Thus, for our devices averaging on the disorder parameters takes place since we measure many QWRs in parallel. Indeed, our temperature dependence measurements (shown below) confirm that the averaging is quite good when we compare samples of the same length but from different growths. Moreover, this setup makes it easier to measure high resistances. A top view scanning electron microscope image of a typical sample is shown in Fig. 1.

The conductance was measured by the four-terminal method using a low-noise analog lock-in amplifier (EG&G PR-124A). The current was passed in two probes ($I+$ and $I-$ in Fig. 1), while the voltage was measured at two different probes ($V+$ and $V-$ in Fig. 1). Notice that all four probes are connected to the 2DEG, so that the contact resistance is always measured, but this resistance is negligible in comparison to the resistances which were measured for the QWRs. The excitation voltage across the sample, V , was always kept below $k_B T/e$. All measurements were done in a ^4He cryogenic system in the temperature range $1.4 < T < 4.2$ K, and approximately half of them were also measured in a dilution refrigerator, allowing us to reach lower temperatures ($T \lesssim 200$ mK). The temperature was measured using a calibrated carbon thermometer (Matsushita 56 resistor).

III. EXPERIMENTAL DATA AND ANALYSIS

For each sample we have measured the conductance as a function of V_G . Figure 2(a) shows such depletion curves for a few typical samples. Here, two points should be discussed: (A) We measure 17 QWRs connected in parallel, so that the depletion curve is somewhat smeared in comparison to the one obtained for a single QWR; (B) since the QWRs are long, they are not ballistic, and the value of the conductance at the first plateau (only one populated channel in each QWR) is much lower than the universal value. Therefore, it is difficult to identify where only one channel is occupying each of the QWRs. To solve these problems, we have chosen the proper gate voltages so that the resistance per QWR per unit length of $1\mu\text{m}$, $\rho_w = 17 \times \frac{R}{L}$ $\text{k}\Omega/\mu\text{m}$ (R is the total resistance), is always larger than the universal value (at $T = 4.2$ K), namely, the resistance of a ballistic segment should always obey the criterion $\rho_w > h/2e^2$. In Fig. 2(a) this criterion is met for $V_G < -2.2$ V.

Next, we measured the conductance of the first plateau (namely, at a certain V_G), for each sample, as a function of temperature. Figure 2(b) shows typical curves of the variation of the conductance (for $\rho_w = 20$ $\text{k}\Omega/\mu\text{m}$) with temperature for various QWR lengths on a log-log scale. As can be seen, $\log_{10} G$ depends linearly on $\log_{10} T$ for all lengths. Moreover, the slope of the shorter samples is smaller than that of the

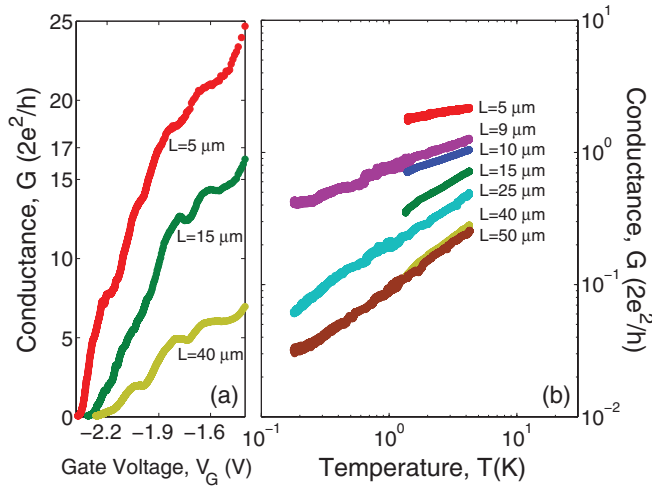


FIG. 2. (Color online) (a) Conductance of 17 QWRs connected in parallel as a function of gate voltage, for samples with lengths 5, 15, and 40 μm . The values of the conductance at the first plateau ($V_G \simeq -2.2$ V) are significantly lower than the ballistic value ($17 \times 2e^2/h$). (b) The value of the conductance of the first plateau (at $\rho_w = 17R/L = 20$ $\text{k}\Omega/\mu\text{m}$) as a function of temperature, for various samples, on a log-log scale.

longer samples. A similar behavior was observed for various values of ρ_w . The observed linear dependence on the log-log scale suggests that the conductance depends on the temperature in a power-law manner, as predicted from the single-barrier theory in Eq. (1). To further substantiate this point, Fig. 3 shows the conductance of the $L = 25$ μm sample as a function of the temperature. As can be seen, an excellent fit is obtained for the single-barrier theory (solid red curve), from which we extract the two fitting parameters $g = 0.62$ and $T_0 = 14$ K. The dashed blue curve represents the best fit for Eq. (3) for the fitting parameter $T_c = 20$ mK. The same analysis was done for

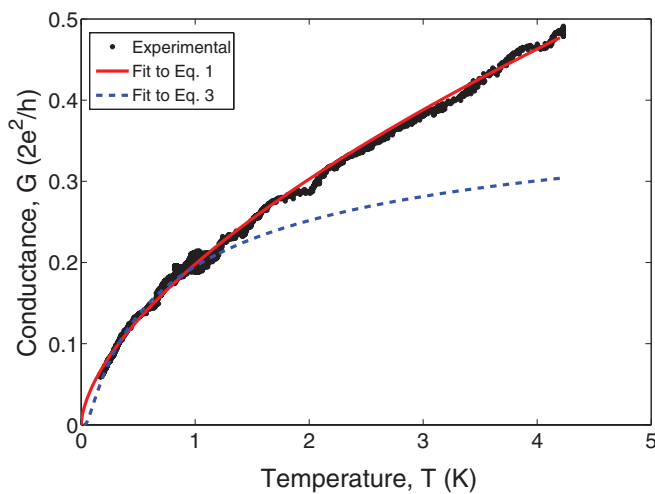


FIG. 3. (Color online) The value of the conductance at the first plateau (at $\rho_w = 17R/L = 20$ $\text{k}\Omega/\mu\text{m}$), for the $L = 25$ μm sample, as a function of temperature (dotted black points). The solid (red) curve represents the fit given by Eq. (1) with the two fitting parameters $g = 0.62 \pm 0.01$ and $T_0 = 14 \pm 0.7$ K. The dashed (blue) curve represents the fit given by Eq. (3) with $T_c = 20$ mK.

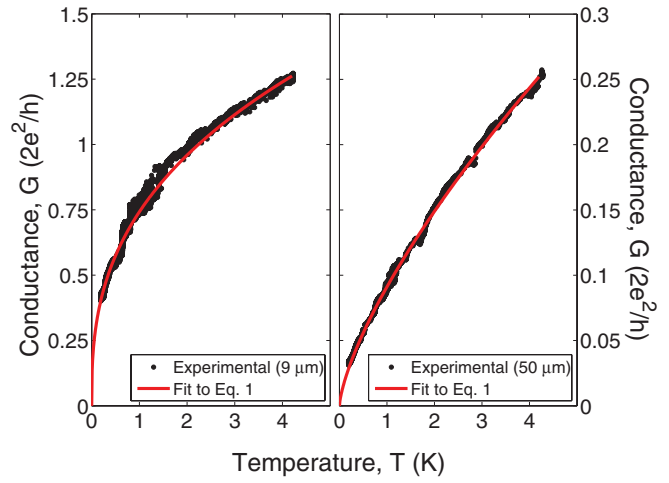


FIG. 4. (Color online) Fits to Eq. (1) (solid red curves) for the lengths 9 μm (left) and 50 μm (right) at $\rho_w = 17R/L = 20$ $\text{k}\Omega/\mu\text{m}$, following the same analysis done for the length 25 μm (see Fig. 3).

all our measured samples. Such fits to Eq. (1) are also shown in Fig. 4 for the lengths 9 and 50 μm .

Figure 5 shows the values of the interaction parameter g and the disorder parameter T_0 which were extracted from the curves obtained for a sample with length $L = 15$ μm , as a function of the applied gate voltage V_G (at values of $\rho_w = 15, 20, 25, 30, 35, 41,$ and 106 $\text{k}\Omega/\mu\text{m}$ as denoted next to each data point). As can be seen, the value of g (blue circles) decreases as gate voltage increases (in magnitude). A similar behavior was observed for all our samples. This is the expected behavior since the electron charge density n_{1D} depends on gate voltage. The larger is the negative gate voltage,

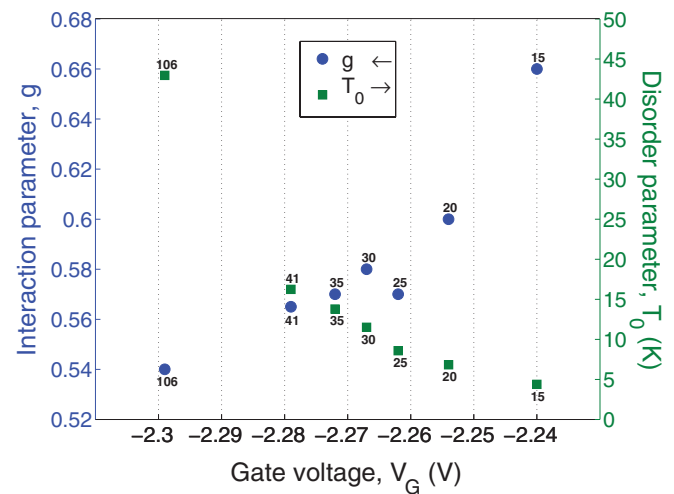


FIG. 5. (Color online) Interaction parameter g (blue circles), and disorder parameter T_0 (green squares) as functions of gate voltage V_G for a 15- μm -long sample. As $|V_G|$ increases, we obtain smaller values of g and higher values of T_0 . This is the expected behavior since the larger is the negative gate voltage, the smaller is the electron charge density n_{1D} . In this case, both e - e interactions and the barrier (effectively) become stronger. Strong interactions correspond to small g , whereas a strong barrier corresponds to large T_0 . The numbers next to the data points are the values of $\rho_w = 17R/L$ in units of $\text{k}\Omega/\mu\text{m}$.

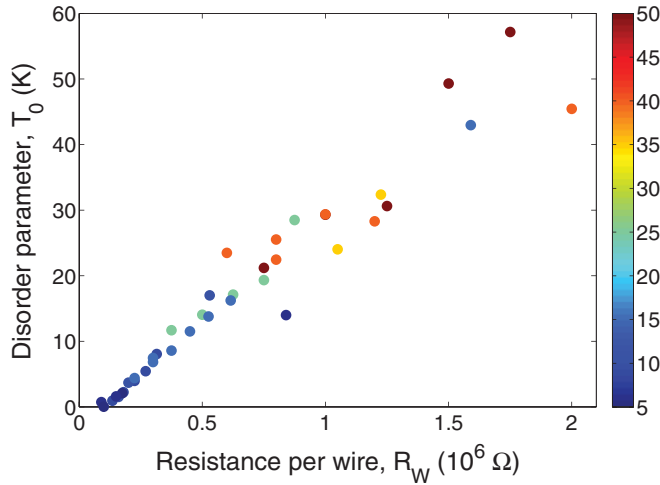


FIG. 6. (Color online) Disorder parameter T_0 as a function of the resistance per wire (at $T = 4.2$ K) R_w . The color bar (grayscale bar) represents the system's length in units of micrometers. R_w is larger for longer samples and increases with negative gate voltage.

the smaller is the electron charge density. Therefore, the value of $2\alpha = U/2E_F$ is greater in Eq. (2),²³ yielding a smaller value of g . On the other hand, the value of T_0 depends on the strength of the barrier. As n_{1D} decreases, the barrier becomes effectively stronger, and T_0 becomes larger, as indeed observed in Fig. 5 (green squares). Moreover, it is reasonable to assume that the value of the disorder parameter T_0 should be larger for longer samples, due to the fact that the probability of finding larger scatterers (stronger barriers) in these systems is bigger. Thus, it is expected that T_0 would increase with R_w , the resistance per wire (at $T = 4.2$ K), since R_w is obviously larger for longer samples and increases with negative gate voltage. This behavior is indeed observed in our samples, as can be seen in Fig. 6.

As has been shown,²³ from each value of the interaction parameter g one can calculate the related Fermi velocity v_F . Figure 7 shows v_F as a function of R_w , for all measured samples. As can be seen, for smaller values of R_w , $v_F \approx 1.5 \times 10^5$ m/s ($\alpha = 0.35$), corresponding to Fermi energies $E_F \approx 4$ meV, which are of the order of the level spacing between 1D subbands in our GaAs QWRs.²⁵ As R_w grows (at higher negative gate voltage and for longer samples), the Fermi energy drops toward the lowest part of the band, and the Fermi velocity is $v_F = 5 \pm 1 \times 10^4$ m/s ($\alpha = 1.06 \pm 0.21$), corresponding to $g = 0.56 \pm 0.04$. The value of the error was chosen from the distribution of the data points in Fig. 7. For these values of $\alpha \sim 1$, all temperature scales become of the same order, $T_c \sim T_1 = T_3 = T_\xi \cong \frac{0.6(\mu\text{m K})}{\xi}$.²⁷ We assume that the localization length in our QWRs is of the order of the maximum length for which the QWRs are still ballistic, namely, $\xi \approx 2\text{--}3 \mu\text{m}$. Therefore, we would expect to see vanishing of the conductance below $T_c \approx 200\text{--}300$ mK. For our samples, trying to fit Eq. (3) to the data yields very low values of $T_c < 50$ mK (as seen in Fig. 3). The exponential dependence is meaningful only for $T - T_c \lesssim T_c$, namely, only at very low temperatures. Therefore, in order to observe this dependence at higher temperatures, one wants to fabricate a sample containing a larger number of scatterers so that ξ will be much smaller.

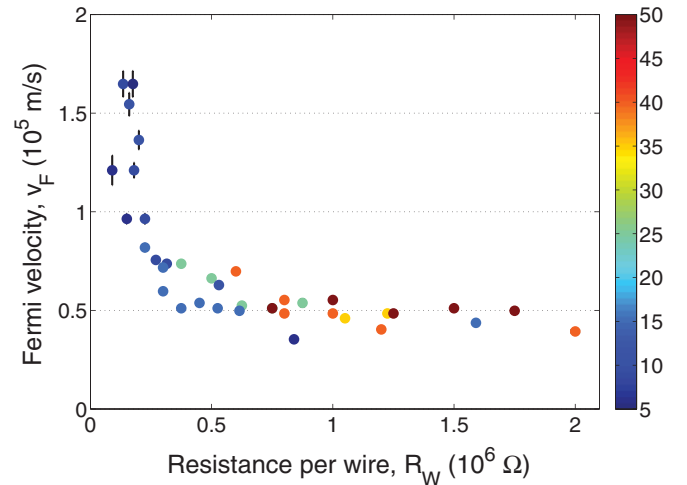


FIG. 7. (Color online) Fermi velocity v_F as a function of the resistance per wire, R_w . The color bar (grayscale bar) represents the system's length in units of micrometers. As can be seen, for large values of R_w the Fermi velocity is $v_F = 5 \pm 1 \times 10^4$ m/s, which corresponds to $g = 0.56 \pm 0.04$. In order to compare between different samples, R_w was used instead of V_G . The reason is that V_G may differ from sample to sample due to different electrostatic properties. R_w depends not only on gate voltage (and therefore on n_{1D}) but also on the system's length [the different colors (grayscale values) represent the lengths, according to the color bar (grayscale bar)]. Nevertheless, the decrease in v_F is associated with the decrease in charge density.

Our data fit Eq. (1) well, which is predicted by the single-barrier LL theory. It is reasonable to assume that in the measured temperature range, $L_\varphi < \xi = 3 \mu\text{m}$, so that on average there is only a single barrier in each segment of length L_φ . An alternative scenario in which many wires are blocked and only few are conducting is very unlikely. The substrates on which the samples are grown are quite homogeneous with respect to disorder (we have measured samples from different growths as well as samples from the same growth but from different locations in the substrate, all showing similar behavior).

IV. SUMMARY

In conclusion, we have measured the temperature dependence of the electrical conductance of sufficiently long GaAs V-groove QWRs occupying a single channel. We find that our data are consistent with theoretical calculations based on the LL model^{8,9} for a single strong barrier. We show that in these QWRs the Fermi velocity can reach a low value of $v_F \cong 5 \times 10^4$ m/s, which corresponds to an interaction parameter value of $g \cong 0.56$.

ACKNOWLEDGMENTS

We thank A. Mirlin, I. Krive, and N.M. Makarov for fruitful discussions. The work was supported by the Israel Science Foundation founded by the Israel Academy of Sciences and Humanities, Grant No. 530/08. The work at EPFL was supported by the Fonds National Suisse de la Recherche Scientifique.

*eyallevy@post.tau.ac.il

- ¹R. Landauer, *Philos. Mag.* **21**, 863 (1970).
- ²B. J. van Wees, H. van Houten, C. W. J. Beenakker, J. G. Williamson, L. P. Kouwenhoven, D. van der Marel, and C. T. Foxon, *Phys. Rev. Lett.* **60**, 848 (1988).
- ³D. A. Wharam, T. J. Thornton, R. Newbury, M. Pepper, H. Ahmed, J. E. F. Frost, D. G. Hasko, D. C. Peacock, D. A. Ritchie, and G. A. C. Jones, *J. Phys. C* **21**, L209 (1988).
- ⁴S. Tomonaga, *Prog. Phys.* **5**, 544 (1950).
- ⁵J. M. Luttinger, *J. Math. Phys.* **4**, 1154 (1963).
- ⁶F. D. M. Haldane, *J. Phys. C* **14**, 2586 (1981).
- ⁷J. von Delft and H. Schoeller, *Ann. Phys. (Berlin)* **7**, 225 (1998).
- ⁸C. L. Kane and M. P. A. Fisher, *Phys. Rev. B* **46**, 15233 (1992).
- ⁹C. L. Kane and M. P. A. Fisher, *Phys. Rev. Lett.* **68**, 1220 (1992).
- ¹⁰M. Ogata and H. Fukuyama, *Phys. Rev. Lett.* **73**, 468 (1994).
- ¹¹D. L. Maslov, *Phys. Rev. B* **52**, R14368 (1995).
- ¹²Y. Oreg and A. M. Finkelstein, *Phys. Rev. B* **54**, R14265 (1996).
- ¹³M. Bockrath, D. H. Cobden, J. Lu, A. G. Rinzler, R. E. Smalley, L. Balents, and P. L. McEuen, *Nature (London)* **397**, 598 (1999).
- ¹⁴Z. Yao, H. W. C. Postma, L. Balents, and C. Dekker, *Nature (London)* **402**, 273 (1999).
- ¹⁵H. Ishii *et al.*, *Nature (London)* **426**, 540 (2003).
- ¹⁶J. Lee, S. Eggert, H. Kim, S.-J. Kahng, H. Shinohara, and Y. Kuk, *Phys. Rev. Lett.* **93**, 166403 (2004).
- ¹⁷E. Levy, A. Tsukernik, M. Karpovski, A. Palevski, B. Dwir, E. Pelucchi, A. Rudra, E. Kapon, and Y. Oreg, *Phys. Rev. Lett.* **97**, 196802 (2006).
- ¹⁸O. M. Auslaender, A. Yacoby, R. de Picciotto, K. W. Baldwin, L. N. Pfeiffer, and K. W. West, *Science* **295**, 825 (2002).
- ¹⁹S. Tarucha, T. Honda, and T. Saku, *Solid State Commun.* **94**, 413 (1995).
- ²⁰I. V. Gornyi, A. D. Mirlin, and D. G. Polyakov, *Phys. Rev. Lett.* **95**, 206603 (2005).
- ²¹P. Fendley, A. W. W. Ludwig, and H. Saleur, *Phys. Rev. B* **52**, 8934 (1995).
- ²²I. V. Gornyi, A. D. Mirlin, and D. G. Polyakov, *Phys. Rev. B* **75**, 085421 (2007).
- ²³The ratio $2\alpha = U/2E_F$ is proportional to v_F^{-1} . Taking $U = (e^2/4\pi\epsilon)n_{1D}$ (where $n_{1D} = 2k_F/\pi = 2mv_F/\pi\hbar$ is the one-dimensional electron charge density) and $E_F = (1/2)mv_F^2$, we get $2\alpha = U/2E_F \simeq 1.06 \times 10^5/v_F$ for our GaAs QWRs.
- ²⁴A. Gustafsson, F. Reinhardt, G. Biasiol, and E. Kapon, *Appl. Phys. Lett.* **67**, 3673 (1995).
- ²⁵D. Kaufman, Y. Berk, B. Dwir, A. Rudra, A. Palevski, and E. Kapon, *Phys. Rev. B* **59**, R10433 (1999).
- ²⁶F. Lelarge, T. Otterburg, D. Y. Oberli, A. Rudra, and E. Kapon, *J. Cryst. Growth* **221**, 551 (2000).
- ²⁷Calculated from $T_\xi = 1/k_B v\xi = \pi\hbar v_F/2k_B\xi$.